

VIETNAM ACADEMY OF SCIENCE AND TECHNOLOGY

Vietnam Journal

of MECHANICS

Volume 36 Number 2

ISSN 0866-7136

VN INDEX 12.666

2

2014

FREE VIBRATION ANALYSIS OF FOUR PARAMETER FUNCTIONALLY GRADED PLATES ACCOUNTING TRANSVERSE SHEAR MODE

Gulshan Taj M. N. A.^{1,*}, Anupam Chakrabarti¹, Mohammad Talha²

¹*Indian Institute of Technology Roorkee, India*

²*International Institute for Aerospace Engineering and Management,
Jain University, India*

*E-mail: gulshantaj19@yahoo.co.in

Received September 24, 2013

Abstract. In the present investigation, free vibration analysis of functionally graded material (FGM) plate is performed incorporating higher order shear deformation theory in conjunction with C_0 based finite element formulation. The cubic component of thickness term is incorporated in in-plane fields and constant variation of thickness is assumed for transverse component. The theory incorporates the realistic parabolic variation of transverse shear stresses thus eliminates the use of shear correction factor. Aluminium/Zirconia plate is considered for the analysis and the effective properties are assumed to have smooth and gradual variation in the thickness direction and remain constant in in-plane direction. The spatial variation of properties pertaining to homogeneous and FGM plate is estimated by means of power law, which is described by the four parameters. With respect to dynamic analysis, it is vital for an analyst to know whether the top of the plate is ceramic or metal rich, and inversely bottom of the plate is ceramic or metal rich. This phenomenon can be described by choosing the appropriate values of the parameters in the power law. In the study, prominence has been given to study the influence of power law parameters on frequency response of FGM plates so as to accomplish different combination of FGM profiles. Thin and moderately thick FGM plates are analyzed to generate the frequency values of the FGM plate. The imperative conclusions presented regarding the choice of parameter in the power law could be useful for designer to arrive for particular material profile of FGM plate.

Keywords: Functionally graded plate, four parameter law, higher order shear deformation theory, free vibration analysis.

1. INTRODUCTION

In view to eliminate the various shortcomings like, delamination, huge stiffness jump and stress discontinuity across the layer interface proffer by conventional composite materials, a new class of materials are in demand by the research community to arrive for optimum and accurate design of structural elements. With regard to this, advanced composite materials with inhomogenous anatomy are discovered by Japan scientists and introduced

to the engineering society to serve under different operating conditions. Typically, FGMs are manufactured by using powder metallurgy techniques, where the two distinct materials are combined to extract their individual superior properties. For the purpose, metal and ceramics are usually united to form FGM structures, which are decidedly applicable in thermal environments e.g., nuclear structures, space shuttles and automotive industries. Moreover, tailoring of FGM material is probable to suit the various practical demands, by virtue of their smooth and gradual variation of properties in the preferred direction. Due to the aforementioned benefits, their vibration response becomes crucial for the safe and optimum design of structure under consideration.

A wide range of publications are recorded in the scientific literature for dynamic analysis of FGM plate and shells concerning various numerical and analytical tools. This is evident from the review article by Jha et al. [1] where the studies related to thermo-elastic static and vibration are discussed briefly based on the various literature data exists since 1998. They noticed that most of the theories developed so far for the analysis of FGM structures considers the transverse shear deformation and the obtained 2D results are usually validated with 3D elasticity solutions. In spite of large number of vibration studies available for FGM plate and shells, only the studies related to the current topic is discussed for the sake of brevity of the presentation. Yang and Shen [2] analyzed the effect of thermal field on free and forced vibration analysis of functionally graded plates. In the study Reddy's higher order shear deformation plate theory is combined with Galerkin technique. They observed that the vibration response of homogeneous plate do not show any intermediate sense, and this tendency is particular when material properties are temperature dependent. Further the authors [3] extended their work to examine the free vibration and stability analysis of FGM cylindrical shell panels under thermo-mechanical environment. Reddy's higher order theory, Galerkin technique and Blotin's method are applied to study the response of the FGM shell panels. Qian et al. [4] presented the static and dynamic analysis of functionally graded plates incorporating higher order shear and normal deformable plate theory. Isvandzibaei and Moarrefzadeh [5] performed the free vibration analysis of FGM shells and influence of different material and geometric parameters on frequency characteristics of shell are discussed in the investigation. Free vibration characteristics of functionally graded cylindrical shell using Reddy's higher order shear deformation theory is performed by Setareh and Isvandzibaei [6]. Static and free vibration analysis of functionally graded material plate considering variation of transverse displacement field is investigated by Talha and Singh [7]. They used variational approach to derive the fundamental equations and considered traction free boundary conditions on the top and bottom faces of the plate to solve for the unknown polynomial terms. Abrate [8] carried out the static, buckling and free vibration analysis of functionally graded plates and pointed out that, the natural frequencies of functionally graded plates are always proportional to those of homogeneous isotropic plates. Uymaz and Aydogdu [9] carried out vibration analysis of FGM plate and they used Chebyshev polynomials to express displacement fields along with Ritz method. Ebrahimi and Rastgo [10] investigated the free vibration behavior of functionally graded circular plates integrated with two uniformly distributed actuator layers made of piezoelectric material based on classical plate theory. In course of time meshless based method attained popularity due to the absence of mesh

technique. In this connection, global collocation method in conjunction with the first and the third-order shear deformation plate theories are used to analyze free vibrations of functionally graded plates by Ferreira et al. [11]. Other studies include vibration analysis of FGM structure under linear, non linear, dynamic and electrical field [12–17]. All the research works so far discussed employs either power law or exponential law to derive the effective properties of ceramic and metal as well. In recent times, Tornabene and his associates [18, 19] incorporated the power law type equation modeled with four parameters for the calculation of material properties. In the research, the author established that different material profiles (metal at top and ceramic at bottom, both top and bottom ceramic, top and bottom are occupied by 50 percent ceramic and 50 percent metal and perhaps other combination also) are possible, by means of appropriate selection of variables. Generalized differential quadrature technique is employed to decompose the governing equations of the plate. A vast number of examples are presented along with the different mode shapes for various types of FGM structures. The kinematic relations are based on the first order shear deformation theory which assumes the linear variation of transverse displacement through the thickness.

It was noticed that some practical design requirements often demands combination of FGM material profiles to meet certain design criteria. Such a demand can be fulfilled by use of suitable general power law distribution reported in the literature that comprises of four parameters to describe the material profile along the thickness direction. The studies so far performed on this topic are based on first order shear deformation theory. For the realistic analysis, it is important to incorporate the actual transverse stress profile in the displacement field. Such an analysis will predict the accurate global response of the plate under loading conditions, in exact sense. To fill this gap, an attempt has been exerted by the authors to study the free vibration analysis of FGM plates using higher order shear deformation theory. A four parameter power law reported in the literature is adopted to estimate the volume fraction of ceramic and metal constituents. Further, the effect of parameters exists in the power law distribution has been studied by performing different numerical examples. Thin and moderately thick plates with different boundary conditions are incorporated in the developed MATLAB (R2011b) code. Conclusions regarding choice of various parameters exist in the power law, type of boundary conditions and thickness ratio could serve as crucial data for researchers involved in FGM analysis. Section 2 elaborates the assumed kinematics field incorporating transverse deformation mode along with the constitutive relationship of FGM material. In Section 3, various numerical examples performed are briefed and to finish, the important key points with respect to the free vibration analysis of four parameter FGM plate are arranged in conclusion part.

2. MATHEMATICAL FORMULATION AND MATERIAL PROPERTIES

2.1. Four parameter power law and constitutive relationship

In general FGM are characterized by their gradual and continuous variation of material properties along the chosen direction (usually thickness direction), hence it is prime factor to capture the accurate particle size distribution in spatial direction. To incorporate this phenomena many methods were addressed and subsequently employed

in the literature by various researchers. Self consistent scheme [20], Mori-Tanaka scheme [21], power law [22], exponential law [23] and sigmoid function [24] are few to cite. Each method has its own superiorities to define the material distribution in a FGM plate. Most of the researchers prefer the power law function to estimate the given material properties [7, 11, 13]. In recent times, Tornabene and his associates [18, 19] established a simple four-parameter power-law and it is given by

$$\text{FGM-I}(a, b, c, p) : V_c = \left(1 - a \left(0.5 + \frac{z}{h} \right) + b \left(0.5 + \frac{z}{h} \right)^c \right)^p \quad (1a)$$

$$\text{FGM-II}(a, b, c, p) : V_c = \left(1 - a \left(0.5 - \frac{z}{h} \right) + b \left(0.5 - \frac{z}{h} \right)^c \right)^p \quad (1b)$$

It is to be noted that, unlike the conventional distribution, the present power law distribution is described by the three parameters a, b, c and power law variable p in the expression. Such a representation would enable the designer to opt for different material profiles such as ceramic at top and metal at bottom, similarly, metal at top and ceramic at bottom and many others. The power law exponent p in the formula assumes the value between zero and infinity to represent different cases of FGM plates. For instance, the value of $p = \text{zero}$, represents homogenous case of ceramic plate, while in other hand the value of $p = \text{infinity}$ resembles the FGM plate occupied by metal segment. The user can vary the range of power law exponent in between zero and infinity to get the plate with gradation properties. Different material combinations of FGM distributions are probable by Eqs. (1a) and (1b), and the type of material distribution depends on choice of the parameters a, b and c . However, the difference of frequency parameters obtained by FGM-I and FGM-II distributions are insignificant and shows deviation after third decimal point (refer the work [18]). Hence in the present work, FGM-I distribution is incorporated to solve the free vibration problem of Al/ZrO₂ plate. Several representations of volume fraction of ceramic are exhibited in Fig. 1. Classical FGM can be achieved by means of choosing $a = 1$ and $b = 0$. Other profiles are obtained by suitably assuming the values of the three parameters a, b and c in the power law formula.

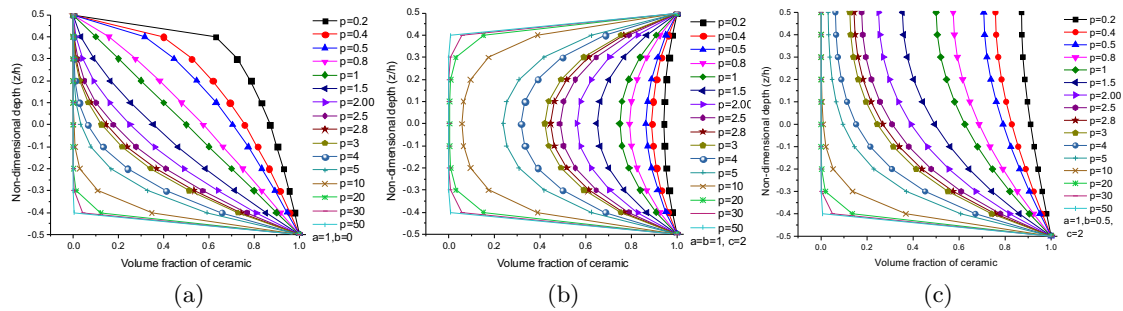


Fig. 1. Different profiles of FGM for several ranges of power law parameters (a) $a = 1, b = 0$ (classical profile) (b) $a = b = 1, c = 2.0$ (symmetric profile) (c) $a = 1, b = 0.5, c = 2.0$

The constitutive relationship of functionally graded plate assuming plane stress condition ($\sigma_{zz} = 0$) may be written as,

$$\begin{pmatrix} \sigma_{xx} \\ \sigma_{yy} \\ \sigma_{yz} \\ \sigma_{xz} \\ \sigma_{xy} \end{pmatrix} = \begin{bmatrix} Q_{11} & Q_{12} & 0 & 0 & 0 \\ Q_{21} & Q_{22} & 0 & 0 & 0 \\ 0 & 0 & Q_{33} & 0 & 0 \\ 0 & 0 & 0 & Q_{44} & 0 \\ 0 & 0 & 0 & 0 & Q_{55} \end{bmatrix} \begin{pmatrix} \varepsilon_{xx} \\ \varepsilon_{yy} \\ \gamma_{yz} \\ \gamma_{xz} \\ \gamma_{xy} \end{pmatrix} \quad (2)$$

$$Q_{11} = Q_{22} = \frac{E(z)}{1 - \gamma^2}, \quad Q_{12} = Q_{21} = \frac{\gamma E(z)}{1 - \gamma^2}, \quad Q_{33} = Q_{44} = Q_{55} = \frac{E(z)}{2(1 + \gamma)}$$

where stiffness co-efficient (Q_{ij}) contains the terms Young's modulus (E) and Poisson's ratio (γ), in which E alone is the function of depth since the properties are assumed as temperature in-dependent.

Utilizing the available expression from Eqs. (1a) and (1b), one can arrive at the material properties of the FGM plate in the following manner.

$$\begin{aligned} E(z) &= E_b + (E_t - E_b) \left(0.5 + \frac{z}{h}\right)^p \\ \rho(z) &= \rho_b + (\rho_t - \rho_b) \left(0.5 + \frac{z}{h}\right)^p \end{aligned} \quad (3)$$

The subscripts 'b' and 't' represent the bottom and top portion of the FGM plate which are usually represented by metal and ceramic, respectively. In the present study, Young's modulus (E) and density (ρ) and treated as position dependent and Poisson's ratio (ν) is assumed to be constant of 0.3. Throughout the analysis, the functional relationship of $V_c + V_m = 1.0$ between the ceramic and metal has to be maintained.

2.2. Displacement function

A Reddy's higher order theory [25] has been implemented in the present study which accounts for the parabolic distribution of transverse shear stresses in the plate. In the theory, the in-plane displacement fields (u and v) are expanded as cubic functions of the thickness coordinate (z), while the transverse displacement (w) variable has been assumed to be constant through the thickness. Any other choice of displacement field would either not satisfy the stress-free boundary conditions or lead to a theory that would involve more dependent unknowns than those in the first-order shear deformation theory [25]. Since the theory assumes the accurate profile of the transverse stress components, the use of shear correction factor could be avoided efficiently. According to Reddy's higher order shear deformation theory [25], the in-plane displacements (u and v) and transverse displacement (w) are expressed in terms of corresponding displacements at the mid surface (u_0, v_0 and w_0) by the following expression.

$$\begin{aligned} u(x, y, z) &= u_0(x, y) + z\theta_x(x, y) + z^2\xi_x(x, y) + z^3\zeta_x(x, y) \\ v(x, y, z) &= v_0(x, y) + z\theta_y(x, y) + z^2\xi_y(x, y) + z^3\zeta_y(x, y) \\ w(x, y) &= w_0(x, y) \end{aligned} \quad (4)$$

where the parameters u_0, v_0 and w_0 are the displacements of points which are in the mid-surface (i.e., reference surface) of the plate and θ_x, θ_y are the bending rotations about the y and x axes respectively. ξ_x, ξ_y, ζ_x and ζ_y are higher order terms appears in Taylor's series

expansion and are solved by the condition of zero transverse shear stains ($\gamma_{xz}(x, y, \pm h/2) = \gamma_{yz}(x, y, \pm h/2) = 0$) at the top and bottom of the plate. After incorporating the necessary boundary conditions the final displacement field turns into following form.

$$\begin{aligned} u(x, y, z) &= u_0(x, y) + z\theta_x - \frac{4z^3}{3h^2} \left(\theta_x + \frac{\partial w}{\partial x} \right) \\ v(x, y, z) &= v_0(x, y) + z\theta_y - \frac{4z^3}{3h^2} \left(\theta_y + \frac{\partial w}{\partial y} \right) \\ w(x, y) &= w_0(x, y) \end{aligned} \quad (5)$$

It is important to mention here that the above form of displacement components represented by Eqs. (5) may invite the problem of C_1 formulation, due to the existence of first order derivatives of transverse components appears in the in-plane field. To overcome the difficulties associated with the C_1 formulation, in the present work, the derivatives of transverse displacement in in-plane displacement fields are replaced by the separate field variables, thus ensuring the C_0 formulation i.e., $\gamma_x = (\theta_x + \frac{\partial w}{\partial x})$ and $\gamma_y = (\theta_y + \frac{\partial w}{\partial y})$. In practice, C_0 elements are preferred rather than C_1 elements and for further details regarding the C_1 and C_0 formulation the reader can refer any standard text book of finite element method [26]. A nine noded Lagrangian element modeled in the study is depicted in Fig. 2. Hence the displacement vector corresponding to each node can be represented as $\{X\} = \{u, v, w, \theta_x, \theta_y, \gamma_x, \gamma_y\}$. Each node has seven nodal unknowns and thus a total of sixty three unknowns are estimated at element level.

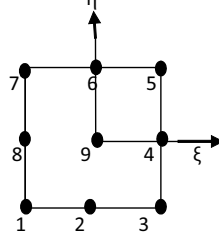


Fig. 2. Lagrangian isoparametric element

The derivations regarding strain-displacement relations and equilibrium equations are briefly discussed by the authors elsewhere [27–29], and not discussed here for the sake of space management.

The governing equation for free vibration analysis is given by,

$$([K] - \omega^2 [M]) \{X\} = \{0\} \quad (6)$$

where $[M]$, $[K]$ and ω are mass matrix, stiffness matrix and frequency parameter derived at element level. The detailed expressions for mass $[M]$ and stiffness matrix $[K]$ are given below.

$$[M] = \iint [C]^T [L] [C] dx dy \quad \text{where} \quad [L] = \int \rho [F]^T [F] dz \quad (7)$$

where matrix $[C]$ and $[F]$ represent the shape functions and thickness co-ordinate terms, respectively, and given in Appendix A.

$$[K] = \iint [B]^T [D] [B] dx dy \quad (8)$$

where $[B]$ is the strain-displacement matrix and $[D]$ represent the rigidity matrix depends on material constitutive properties in Eq. (2). The corresponding strain-displacement relation is given in Appendix B.

The right hand side zero of the Eq. (6) represents the problem of free vibration analysis. The mass and stiffness matrices formed at element level are assembled to get stiffness matrix at global domain. This can be achieved by taking the contribution of all the plate elements. The skyline storage scheme is used to store the elements in global stiffness matrix. A standard eigen value algorithm is utilized to extract the mode shapes of the FGM plate. The detailed steps involved in the algorithm are given in Appendix C.

3. NUMERICAL RESULTS AND DISCUSSION

A computer code is developed in MATLAB environment based on the above formulation that accounts for the realistic parabolic variation of transverse stresses through the thickness. For the purpose of generating results, Aluminium/Zirconia plate is considered for all the numerical examples performed, unless otherwise specified. It is to be noted that, the bottom of the plate is enriched with Aluminium, while the top of the plate is made of Zirconia. The material properties of the FGM plate are: $E = 168$ GPa, $\rho = 5700$ kg/m³ for Zirconia (ceramic), and $E = 70$ GPa, $\rho = 2707$ kg/m³ for Aluminium (metal). Since the effect of Poisson's ratio on deflection is insignificant [26], a constant value of 0.3 is assumed for both the materials. A square plate ($a = b = 1$ m) is considered with different boundary conditions (simply supported, clamped and simply supported-clamped) to tabulate the results. To study the influence of parameters a, b, c and p that appears in Eq. (1a), thin ($h = 0.01$) and moderately thick ($h = 0.1$) plates are assumed in the numerical part. The present formulation has been validated for number of analyses with respect to rectangular and skew FGM plates and reported by authors in their earlier works [27–29]. In the present study, the prominence has been exerted to study the influence of parameters a, b, c and p on frequency of FGM plate. Such a topic could able the designer to choose the appropriate value of power law parameters to solve for real time applications.

The values of first six natural frequencies for simply supported thin and moderately thick FGM plate is furnished in Tabs. 1 and 2, respectively. Three types of power law profiles are considered for each case for example, classic, symmetric and asymmetric. The exact values of power law parameters (a, b and c) chosen for each case are furnished in Fig. 1. The value of power law exponents ranges from p ($0 < p < 20$). The case of $p = 0$, represents the homogenous case of ceramic plate. In both Tab. 1 and Tab. 2, it is manifested that the elevation of power law exponent from homogeneous to FGM plate increases the frequency of FGM plate. This trend is observed as common phenomenon in all the three profiles (classical, symmetric and asymmetric). The reason attributed is that the increase in metal content corresponds to low stiffness thus reducing the frequency as the power law exponent rises. Further for all the three profiles considered, the value of

$p = 0$, produces the same frequency, due to the isotropic property of plate. In Tab. 1, the symmetric profile exhibits high frequency value followed by asymmetric and classical profiles, when the power law exponent ranges from 0 to 1. Beyond the linear range ($p > 1$), the classical FGM plates produces higher frequency, thus ensuring the high stiffness of the plate under consideration. The low values of frequencies are recorded for thin plate compared to moderately thick plates as expected, considering different values of power law exponent. The observations regarding the influence of chosen profile on frequency extracted from Tab. 1 are analogous for Tab. 2 also. Since the symmetric profile of FGM plate ensures the ceramic segment at top and bottom of the plate (refer Fig. 1(a)) having high stiffness, shows better performance compared with other two cases of FGM profiles.

Table 1. Natural frequencies of four-parameter FGM plate for first six modes (simply supported, $h = 0.1$)

p	0	0.2	0.4	1	5	10	20
Classic	324.1771	323.3509	322.4659	319.5509	287.9179	200.7168	64.20281
	810.0952	808.0331	805.8241	798.5465	719.5333	501.6757	160.5009
	1295.472	1292.178	1288.65	1277.022	1150.724	802.4174	256.7668
	1619.64	1615.526	1611.117	1596.589	1438.734	1003.339	321.1017
Symmetric	324.1771	324.9004	325.5331	326.7571	282.8979	138.2552	23.62688
	810.0952	811.9001	813.4788	816.5307	706.9492	345.567	59.06632
	1295.472	1298.354	1300.875	1305.744	1130.537	552.74	94.49552
	1619.64	1623.24	1626.388	1632.467	1413.444	691.1558	118.1739
Asymmetric	324.1771	323.6979	323.145	321.0901	287.5848	187.9573	51.54532
	810.0952	808.8992	807.5188	802.3878	718.6918	469.7836	128.8586
	1295.472	1293.561	1291.356	1283.157	1149.364	751.4057	206.1462
	1619.64	1617.253	1614.498	1604.253	1437.022	939.5536	257.798

Table 2. Natural frequencies of four-parameter FGM plate for first six modes (simply supported, $h = 0.01$)

p	0	0.2	0.4	1	5	10	20
Classic	3132.852	3125.462	3117.48	3090.867	2793.455	1963.022	635.5957
	7481.315	7465.368	7447.947	7388.901	6703.212	4757.477	1565.769
	10577.5	10575.27	10574.15	10577.09	10339.33	7397.019	2469.472
	10577.5	10575.27	10574.15	10577.09	10755.76	9086.254	3059.584
Symmetric	3132.852	3139.264	3144.812	3155.066	2735.686	1354.249	234.2482
	7481.315	7494.977	7506.619	7526.66	6537.607	3287.879	578.2702
	10577.5	10580.63	10584.62	10601.7	10049.83	5118.174	913.7849
	10577.5	10580.63	10584.62	10601.7	10853.49	6290.415	1133.513
Asymmetric	3132.852	3128.547	3123.524	3104.584	2788.14	1838.044	510.3354
	7481.315	7471.966	7460.891	7418.333	6684.272	4453.685	1257.335
	10577.5	10576.15	10575.84	10580.93	10302.35	6922.942	1983.185
	10577.5	10576.15	10575.84	10580.93	10773.04	8502.296	2457.191

Table 3. Natural frequencies of four-parameter FGM plate for first six modes (clamped, $h = 0.1$)

p	0	0.2	0.4	1	5	10	20
Classic	5351.332	5340.513	5328.595	5287.73	4800.356	3412.43	1129.664
	10228.3	10210.51	10190.54	10120.19	9231.368	6643.842	2248.666
	14361.95	14339.35	14313.63	14221.47	13013.22	9442.17	3246.746
	16951.14	16926.57	16898.25	16795.22	15401.39	11234.82	3903.099
Symmetric	5351.332	5360.513	5368.242	5380.771	4667.175	2355.196	417.5748
	10228.3	10243.06	10255.12	10271.63	8927.615	4593.57	833.7104
	14361.95	14380.41	14395.17	14412.54	12546.16	6535.852	1206.544
	16951.14	16970.9	16986.37	17001.59	14812.36	7780.121	1452.583
Asymmetric	5351.332	5344.962	5337.332	5307.609	4783.676	3192.332	907.0319
	10228.3	10217.71	10204.7	10152.5	9188.311	6212.726	1805.685
	14361.95	14348.39	14331.45	14262.16	12943.47	8827.05	2607.327
	16951.14	16936.28	16917.44	16839.1	15310.54	10499.89	3134.476

Table 4. Natural frequencies of four-parameter FGM plate for first six modes (clamped, $h = 0.01$)

p	0	0.2	0.4	1	5	10	20
Classic	590.5254	589.0234	587.4141	582.1116	524.5195	365.718	117.0151
	1203.612	1200.557	1197.284	1186.493	1069.19	745.6393	238.6523
	1773.148	1768.657	1763.843	1747.97	1575.276	1098.792	351.7923
	2157.098	2151.64	2145.789	2126.494	1916.483	1336.935	428.1054
Symmetric	590.5254	591.84	592.9895	595.2106	515.3173	251.9106	43.06357
	1203.612	1206.285	1208.622	1213.131	1050.323	513.6197	87.83163
	1773.148	1777.077	1780.51	1787.127	1547.327	756.9039	129.4756
	2157.098	2161.872	2166.043	2174.078	1882.394	920.9689	157.5654
Asymmetric	590.5254	589.6541	588.6485	584.9095	523.9001	342.465	93.94575
	1203.612	1201.84	1199.794	1192.183	1067.903	698.2254	191.6026
	1773.148	1770.543	1767.533	1756.334	1573.345	1028.915	282.4378
	2157.098	2153.931	2150.273	2136.658	1914.115	1251.913	343.7065

The free vibration results of Aluminium/Zirconia thin and moderately thick plate with clamped boundary is furnished in Tabs. 3 and 4, respectively. Because of the high bending nature of the clamped boundary, the higher values of frequency are reported for both the cases. The observations regarding the profile type on natural frequencies drawn from Tabs. 1 and 2 holds true for Tabs. 3 and 4 also, except the frequency values are higher for the later case. In Tabs. 5 and 6, the simply supported-clamped FGM plates are considered to generate the frequency values. Intermediate values of frequency are recorded, since two of the edges correspond to simply-supported boundary, thereby reducing the total stiffness of the plate. Once again, symmetric profile is turned to be a better choice compared with classical and asymmetric profiles, by virtue of high stiffness at top and bottom of the plate. Further to show the influence of each parameter on frequency, three examples are illustrated. In all the cases, one of the parameter is varied, whilst remaining

two parameters are treated as constant. The value of power law exponent is varied from 0 to 100.

Table 5. Natural frequencies of four-parameter FGM plate for first six modes (simply supported- clamped, $h = 0.1$)

p	0	0.2	0.4	1	5	10	20
Classic	4156.973	4147.89	4137.986	4104.511	3718.128	2628.357	860.5396
	8792.393	8775.471	8756.735	8692.041	7908.192	5654.128	1887.878
	12051.01	12048.47	12047.17	12050.42	11642.45	8391.26	2844.406
	12893.85	12871.23	12845.91	12757.06	12251.44	10163.68	3476.406
Symmetric	4156.973	4164.77	4164.77	4183.034	3627.797	1813.751	317.6164
	8792.393	8806.671	8806.671	8837.217	7678.918	3908.736	698.6065
	12051.01	12054.58	12054.58	12078.47	11268.46	5807.666	1054.814
	12893.85	12912.67	12912.67	12949.89	12360.48	7037.288	1290.834
Asymmetric	4156.973	4151.655	4145.37	4121.291	3708.067	2459.947	690.9498
	8847.72	8837.613	8825.438	8777.686	7926.335	5319.885	1523.394
	12051.01	12049.47	12049.1	12054.79	11589.97	7848.985	2284.268
	12893.85	12880.4	12863.95	12798.19	12270.74	9504.534	2791.885

Table 6. Natural frequencies of four-parameter FGM plate for first six modes (simply supported-clamped, $h = 0.01$)

p	0	0.2	0.4	1	5	10	20
Classic	444.1443	443.0135	441.802	437.8109	394.4827	275.0275	87.98444
	993.2975	990.7727	988.0675	979.1529	882.3082	615.2365	196.8725
	1522.186	1518.323	1514.183	1500.538	1352.21	943.0533	301.8472
	1878.978	1874.214	1869.109	1852.276	1669.238	1164.262	372.7016
Symmetric	444.1443	445.1342	446.000	447.6739	387.5844	189.4415	32.37916
	993.2975	995.5071	997.4393	1001.171	866.8104	423.7926	72.45336
	1522.186	1525.566	1528.52	1534.222	1328.358	649.6201	111.0897
	1878.978	1883.147	1886.79	1893.817	1639.73	802.0132	137.1686
Asymmetric	444.1443	443.4884	442.7314	439.9176	394.0218	257.5425	70.63843
	993.2975	991.833	990.1423	983.856	881.2617	576.1202	158.0596
	1522.186	1519.945	1517.357	1507.733	1350.583	883.0914	242.3392
	1878.978	1876.215	1873.023	1861.15	1667.216	1090.233	299.2252

Fig. 3 depicts the free vibration results of FGM plate in which the parameters b and c are kept constant and the parameter a is varied from 0 to 1.2. In all the cases, a ceramic line is established which contributes high stiffness to the plate. A fast descending behavior of frequency is discerned as the plate turned from isotropic to FGM case. Because the increase in value of power law exponent tends to reduce the stiffness of the plate further for all cases. In some cases, the natural frequency of FGM plate exceeds the limit case of ceramic plate. For particular, in frequency mode 5 and 6, lower value of the parameter a (0.2 to $\cong 0.8$) exceeds the maximum frequency of the plate. This is due to the choice of parameter b and c to decide the frequency value. In particular, the types of vibration

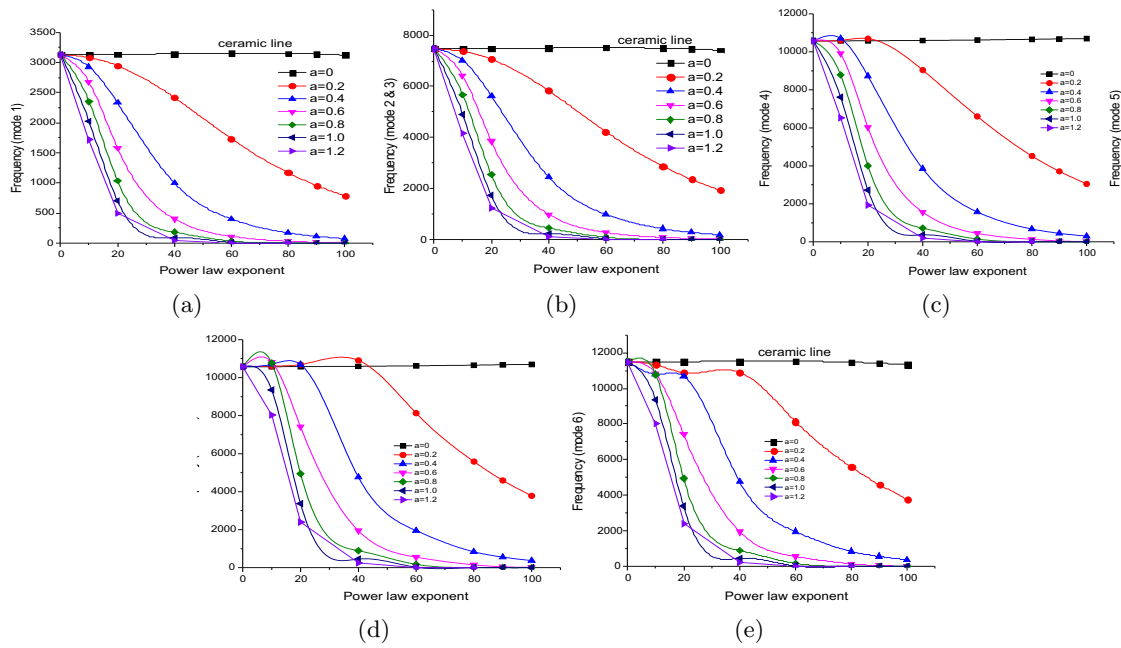


Fig. 3. First six natural frequencies of FGM plate ($0 < a < 1.2$)

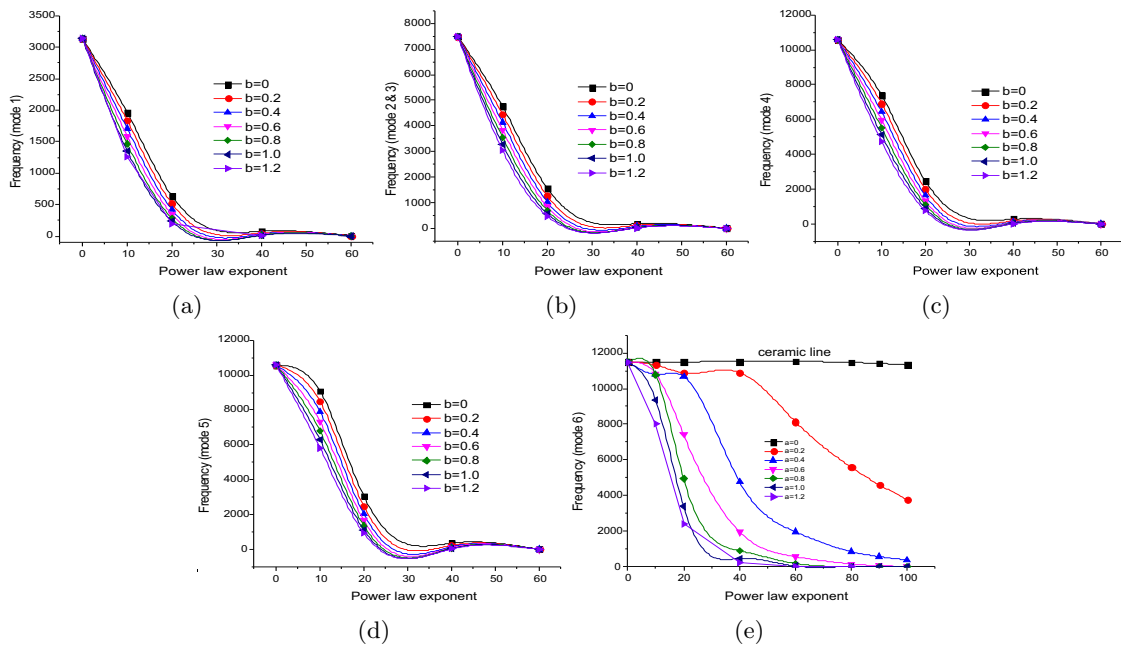


Fig. 4. First six natural frequencies of FGM plate ($0 < b < 1.2$)

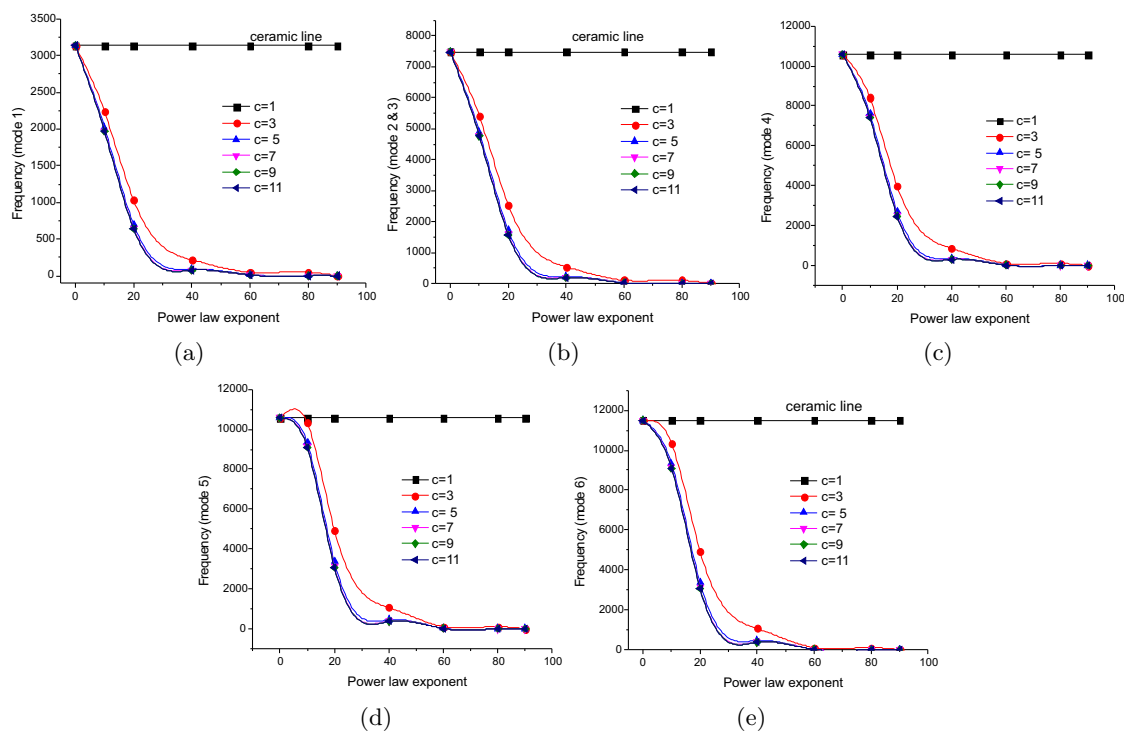


Fig. 5. First six natural frequencies of FGM plate ($1 < c < 11$)

mode that ensures this type of monotone decrease of frequency are torsional, bending and axisymmetric mode shapes. In Fig. 4, the parameter b is varied from 0 to 1.2 while other two parameters are kept constant. A convex type of descending behavior is discerned in all the type of frequency modes. For homogeneous case of plate, all the cases merge at same frequency value. Beyond certain value of power law exponent (say $p \cong 25$), the frequency of plate considering different values of the parameter b establishes stable path. Hence it can be inferred that change in value of the parameter b has no significant effect beyond certain value of p . The first six mode shapes of FGM plate for several ranges of the power law parameter c is exhibited in Fig. 5. The value of $c = 1$, establishes the ceramic line corresponds to high stiffness of the plate. For further value of c ($c = 3, 7, 9$ and 11), a steep tendency of frequency value is noticed. Exceeding the power law exponent beyond 40, shows stable point for all the cases of c considered, except for the case $c = 1$. Further in mode 5, the value of the parameter c corresponds to 3, exceeds the limit case of ceramic plate due to the choice of the other parameters a and b . This behavior depends on the type of vibration mode and value of the parameter c .

4. CONCLUSIONS

An efficient C_0 based finite element formulation is presented for free vibration response of four-parameter functionally graded plates in conjunction with higher order shear

deformation theory. Four parameter based power law function is utilized in order to estimate the volume fraction of ceramic and metal components. The four parameters exists in the power law expression describes the various material profile of functionally graded plate along the thickness direction. To perform the numerical examples various combination of parameters are considered. Natural frequencies of free vibration of FGM plate are presented in the form of tables and figures.

Classical, symmetric and asymmetric profiles are generated by the suitable assumption of value of power law parameters. It was noticed symmetric profiles exhibits maximum frequency value for certain value of power law exponent ($p > 1$) and this tendency is irrespective of the plate thickness and boundary condition. Variation of single parameter in a power function leads to fall-off in frequency parameter when the power law exponent rises. Due to the choice of other two parameters in the power function, for certain types of modes, the plate with gradation properties records frequency greater than homogenous ceramic plate. For a designer it is vital to acquire the knowledge about the material distribution of plate (either ceramic or metal) at the top and bottom to meet the practical demands. Henceforth, the free vibration of FGM plate based on four-parameter power law could serve as key topic from dynamic point of view.

REFERENCES

- [1] D. Jha, T. Kant, and R. Singh. A critical review of recent research on functionally graded plates. *Composite Structures*, **96**, (2013), pp. 833–849.
- [2] J. Yang and H.-S. Shen. Vibration characteristics and transient response of shear-deformable functionally graded plates in thermal environments. *Journal of Sound and Vibration*, **255**, (3), (2002), pp. 579–602.
- [3] J. Yang and H.-S. Shen. Free vibration and parametric resonance of shear deformable functionally graded cylindrical panels. *Journal of Sound and Vibration*, **261**, (5), (2003), pp. 871–893.
- [4] L. Qian, R. Batra, and L. Chen. Static and dynamic deformations of thick functionally graded elastic plates by using higher-order shear and normal deformable plate theory and meshless local Petrov-Galerkin method. *Composites Part B: Engineering*, **35**, (6), (2004), pp. 685–697.
- [5] M. R. Isvandzibaei and A. Moarrefzadeh. Vibration two type functionally graded cylindrical shell. *Int. J. Multidisciplinary Sciences and Engineering*, **2**, (8), (2011), pp. 7–11.
- [6] M. Setareh and M. R. Isvandzibaei. A finite element formulation for analysis of functionally graded plates and shells. *J. Basic and Applied Scientific Research*, **1**, (2011), pp. 1236–1243.
- [7] M. Talha and B. Singh. Static response and free vibration analysis of FGM plates using higher order shear deformation theory. *Applied Mathematical Modelling*, **34**, (12), (2010), pp. 3991–4011.
- [8] S. Abrate. Free vibration, buckling, and static deflections of functionally graded plates. *Composites Science and Technology*, **66**, (14), (2006), pp. 2383–2394.

- [9] B. Uymaz, M. Aydogdu, and S. Filiz. Vibration analyses of FGM plates with in-plane material inhomogeneity by Ritz method. *Composite Structures*, **94**, (4), (2012), pp. 1398–1405.
- [10] F. Ebrahimi and A. Rastgo. Free vibration analysis of smart FGM plates. *International Journal of Mechanical Systems Science & Engineering*, **2**, (2008), pp. 94–98.
- [11] A. Ferreira, R. Batra, C. Roque, L. Qian, and R. Jorge. Natural frequencies of functionally graded plates by a meshless method. *Composite Structures*, **75**, (1), (2006), pp. 593–600.
- [12] J. Woo and S. Meguid. Nonlinear analysis of functionally graded plates and shallow shells. *International Journal of Solids and structures*, **38**, (42), (2001), pp. 7409–7421.
- [13] J. S. Kumar, B. S. Reddy, C. E. Reddy, and K. Reddy. Higher order theory for free vibration analysis of functionally graded material plates. *Journal of Engineering & Applied Sciences*, **6**, (10), (2011), pp. 105–111.
- [14] S. M. Hasheminejad and A. Rafsanjani. Three-dimensional vibration analysis of thick FGM plate strips under moving line loads. *Mechanics of Advanced Materials and Structures*, **16**, (6), (2009), pp. 417–428.
- [15] G. Praveen and J. Reddy. Nonlinear transient thermoelastic analysis of functionally graded ceramic-metal plates. *International Journal of Solids and Structures*, **35**, (33), (1998), pp. 4457–4476.
- [16] H. Matsunaga. Free vibration and stability of functionally graded plates according to a 2-D higher-order deformation theory. *Composite structures*, **82**, (4), (2008), pp. 499–512.
- [17] C.-S. Chen, C.-Y. Hsu, and G. J. Tzou. Vibration and stability of functionally graded plates based on a higher-order deformation theory. *Journal of Reinforced Plastics and Composites*, **28**, (10), (2009), pp. 1215–1234.
- [18] F. Tornabene. Free vibration analysis of functionally graded conical, cylindrical shell and annular plate structures with a four-parameter power-law distribution. *Computer Methods in Applied Mechanics and Engineering*, **198**, (37), (2009), pp. 2911–2935.
- [19] F. Tornabene and E. Viola. Static analysis of functionally graded doubly-curved shells and panels of revolution. *Meccanica*, **48**, (4), (2013), pp. 901–930.
- [20] R. Hill. A self-consistent mechanics of composite materials. *Journal of the Mechanics and Physics of Solids*, **13**, (4), (1965), pp. 213–222.
- [21] T. Mori and K. Tanaka. Average stress in matrix and average elastic energy of materials with misfitting inclusions. *Acta metallurgica*, **21**, (5), (1973), pp. 571–574.
- [22] S. Suresh, A. Mortensen, and S. Suresh. *Fundamentals of functionally graded materials*. Institute of Materials London, (1998).
- [23] Z.-H. Jin and R. Batra. Stress intensity relaxation at the tip of an edge crack in a functionally graded material subjected to a thermal shock. *Journal of Thermal Stresses*, **19**, (4), (1996), pp. 317–339.
- [24] Y. Chung and S. Chi. The residual stress of functionally graded materials. *J Chin Inst Civil Hydraulic Eng*, **13**, (2001), pp. 1–9.
- [25] J. N. Reddy. A simple higher-order theory for laminated composite plates. *Journal of Applied Mechanics*, **51**, (4), (1984), pp. 745–752.

- [26] C. Krishnamoorthy. *Finite element analysis: Theory and programming*. Tata McGraw-Hill Education, (1994).
- [27] M. Gulshan Taj and A. Chakrabarti. Static and dynamic analysis of functionally graded skew plates. *Journal of Engineering Mechanics*, **139**, (7), (2012), pp. 848–857.
- [28] M. Gulshan Taj, A. Chakrabarti, and A. H. Sheikh. Analysis of functionally graded plates using higher order shear deformation theory. *Applied Mathematical Modelling*, **37**, (18), (2013), pp. 8484–8494.
- [29] M. Gulshan Taj and A. Chakrabarti. Dynamic response of functionally graded skew shell panel. *Latin American Journal of Solids and Structures*, **10**, (6), (2013), pp. 1243–1266.

APPENDIX A

$C(1, 1) = N_1; C(1, 8) = N_2; C(1, 15) = N_3; C(1, 22) = N_4; C(1, 29) = N_5; C(1, 36) = N_6; C(1, 43) = N_7; C(1, 50) = N_8; C(1, 57) = N_9$ and all other terms of the row one will be zero. Similarly, all other row values are obtained according to each degree of freedom. The detailed expression for shape functions for the assumed Lagrangian element is presented below.

$$\begin{aligned} N_1 &= \frac{1}{4}(\xi - 1)(\eta - 1)\xi\eta, N_2 = \frac{1}{4}(\xi + 1)(\eta - 1)\xi\eta, N_3 = \frac{1}{4}(\xi + 1)(\eta + 1)\xi\eta, \\ N_4 &= \frac{1}{4}(\xi - 1)(\eta + 1)\xi\eta, N_5 = -\frac{1}{2}(1 - \xi^2)(1 - \eta)\eta, N_6 = -\frac{1}{2}(1 + \xi)(\eta^2 - 1)\xi, \quad (\text{A.1}) \\ N_7 &= -\frac{1}{2}(\xi^2 - 1)(1 + \eta)\eta, N_8 = -\frac{1}{2}(\xi - 1)(\eta^2 - 1)\xi, N_9 = (1 - \xi^2)(1 - \eta^2). \end{aligned}$$

where ξ and η represents the natural co-ordinate system of the element (Fig. 2).

$$[F] = \begin{bmatrix} 1 & 0 & 0 & z & 0 & \frac{-4z^3}{3h^2} & 0 \\ 0 & 1 & 0 & 0 & z & 0 & \frac{-4z^3}{3h^2} \\ 0 & 0 & 1 & 0 & 0 & 0 & 0 \end{bmatrix}. \quad (\text{A.2})$$

APPENDIX B

By utilizing the displacement components given in Eqs. (5) the mechanical strain at a point can be represented as

$$\{\varepsilon_m\} = \left\{ \begin{array}{l} \frac{\partial u}{\partial x} \\ \frac{\partial v}{\partial y} \\ \frac{\partial u}{\partial y} + \frac{\partial v}{\partial x} \\ \frac{\partial u}{\partial z} + \frac{\partial w}{\partial x} \\ \frac{\partial v}{\partial z} + \frac{\partial w}{\partial y} \end{array} \right\} = \left\{ \begin{array}{l} \frac{\partial u_0}{\partial x} + z \frac{\partial \theta_x}{\partial x} - \frac{4z^3}{3h^2} \frac{\partial \gamma_x}{\partial x} \\ \frac{\partial v_0}{\partial y} + z \frac{\partial \theta_y}{\partial y} - \frac{4z^3}{3h^2} \frac{\partial \gamma_y}{\partial y} \\ \frac{\partial u_0}{\partial y} + z \frac{\partial \theta_x}{\partial x} - \frac{4z^3}{3h^2} \frac{\partial \gamma_x}{\partial x} + \frac{\partial v_0}{\partial y} + z \frac{\partial \theta_y}{\partial y} - \frac{4z^3}{3h^2} \frac{\partial \gamma_y}{\partial y} \\ \frac{\partial w_0}{\partial x} + \theta_x - \frac{4z^2}{h^2} \gamma_x \\ \frac{\partial w_0}{\partial y} + \theta_y - \frac{4z^2}{h^2} \gamma_y \end{array} \right\} \quad (\text{B.1})$$

Mechanical strain in terms of total strain can be rewritten as $\{\varepsilon_m\} = [H] \{\varepsilon\}$

The strain matrix $\{\varepsilon\}$ can be written in terms of nodal displacement vector $\{X\}$ by means of strain-displacement matrix $[B]$. The components of matrix $[B]$ involve derivatives of shape function terms and having the matrix order of 15×63 .

APPENDIX C

The stiffness matrix $[K]$ in Eq. (6) is positive definite and can be decomposed into Cholesky factors as

$$[K] = [L][T]^T \quad (\text{C.1})$$

where $[L]$ is the lower triangular matrix. Using Eq. (6), Eq. (C.1) is rewritten for the free vibration analysis as:

$$\{[L]^{-1}[M][L]^{-T}\}[L]^T\{X\} = \frac{1}{\omega^2}[L]^T\{X\} \quad (\text{C.2})$$

The Eq. (C.2) represents standard eigen value problem and this has been solved to extract the eigen values and the eigen vectors. The term $1/\omega^2$ appear in Eq. (C.2) is the eigen value. The eigen value corresponding to the lowest natural frequency is obtained using the simultaneous iteration technique. The detailed methodology is explained as follows:

- (i) Set a trial vector $[U]$ and ortho-normalize.
- (ii) Back substitute $[L][X] = [U]$
- (iii) Multiply $[Y] = [M][X]$
- (iv) Forward substitute $[L]^T[V] = [Y]$
- (v) Form $[B] = [U]^T[V]$
- (vi) Construct $[T]$ so that $t_{ij} = 1$ and $t_{ij} = \frac{-2b_{ij}}{[b_{ii} - b_{ij} + s(b_{ii} - b_{ij})^2]}$, where s is the sign of $(b_{ii} - b_{ij})$
- (vii) Multiply $[W] = [V][T]$
- (viii) Perform Schmidt ortho-normalization to derive $[\bar{U}]$
- (ix) Check tolerance $[U] - [\bar{U}]$
- (x) If not satisfactory, go to step (ii).

CONTENTS

	Pages
1. Dao Huy Bich, Nguyen Dang Bich, A coupling successive approximation method for solving Duffing equation and its application.	77
2. Nguyen Thai Chung, Hoang Xuan Luong, Nguyen Thi Thanh Xuan, Dynamic stability analysis of laminated composite plate with piezoelectric layers.	95
3. Vu Le Huy, Shoji Kamiya, A direct evidence of fatigue damage growth inside silicon MEMS structures obtained with EBIC technique.	109
4. Nguyen Tien Khiem, Duong The Hung, Vu Thi An Ninh, Multiple crack identification in stepped beam by measurements of natural frequencies.	119
5. Nguyen Hong Son, Hoang Thi Bich Ngoc, Dinh Van Phong, Nguyen Manh Hung, Experiments and numerical calculation to determine aerodynamic characteristics of flows around 3D wings.	133
6. Gulshan Taj M. N. A., Anupam Chakrabarti, Mohammad Talha, Free vibration analysis of four parameter functionally graded plate accounting for realistic transverse shear mode.	145